Eur Biophys J (1993) 22:157–167

European Biophysics Journal

Low temperature optical spectroscopy of cobalt-substituted hemocyanin from *Carcinus maenas*

Eugenio Vitrano [1], Antonio Cupane [1], Maurizio Leone [1], Valeria Militello [1], Lorenzo Cordone [1], Benedetto Salvato [2, 3], Mariano Beltramini [2, 3], Luigi Bubacco [2,*], Gian Paolo Rocco [3]

[1] Istituto di Fisica dell'Università di Palermo and GNSM-JNFM, via Archirafi 36, I-90123 Palermo, Italy
[2] Dipartimento di Biologia dell'Università di Padova, via Trieste 75, I-35121 Padova, Italy
[3] CNR Centro per le Emocianine e altre metalloproteine, via Trieste 75, I-35121 Padova, Italy

Received: 13 November 1992 / Accepted in revised form: 9 April 1993

Abstract. In this work we report the optical absorption spectra of three cobalt-substituted derivatives of hemocyanin (Hc) from *Carcinus maenas*, in the temperature range 300–20 K. The derivatives studied are the mononuclear (Co^{2+})-Hc with a single cobalt ion in the "Cu_A" site, the binuclear $(Co^{2+})_2$-Hc and the binuclear mixed metal $(Co^{2+}$-$Cu^{1+})$-Hc. At low temperature three main bands are clearly resolved; the temperature dependence of their zeroth, first and second moments sheds light on the stereodynamic properties in the surroundings of the chromophore. Within the limits of the reported analysis, in the binuclear derivatives the motions coupled to the chromophore appear to be "essentially harmonic" in the whole temperature range investigated; moreover the data are consistent with the presence of an exogenous ligand strongly bound to the two metal ions. For the mononuclear derivative an "essentially harmonic" behavior is evident only up to 200 K where the data are consistent with the presence of an exogenous ligand much less strongly bound, while at higher temperatures the behavior of the spectra indicates the onset of very large anharmonic contributions to motions, that plausibly involve the above exogenous ligand and, quite likely, the entire active site.

Key words: Hemocyanin – Optical spectra – Vibrational coupling

Introduction

Hemocyanins[1] (Hcs), the oligomeric copper containing proteins found in the hemolymph of several molluscs and arthropods, possess a binuclear coupled copper active site specialized in the reversible binding of molecular dioxygen (Solomon 1981; Solomon et al. 1992).

X-ray diffraction data, up to now available for the deoxygenated form of *Panulirus interruptus* Hc at 3.2 Å resolution (Gaykema et al. 1984; Volbeda and Hol 1989; Hol et al. 1990), give an essentially symmetric picture of this site; the two copper ions are located in an hydrophobic pocket surrounded by non polar aliphatic aminoacid side chains, deeply imbedded in the protein matrix and shielded from interaction with the external medium. Each metal is bound by three imidazole N1 nitrogens, two of which are at about 2.0 Å bonding distance, whilst the third one is at the longer distance of about 2.7 Å. The four nitrogens at shorter distance, together with the two copper ions, are almost coplanar, whereas the other two nitrogens lie on the opposite sides of this plane. The copper-copper distance is 3.6 Å.

This highly symmetric binuclear cuprous site still maintains its symmetry upon binding molecular dioxygen. Upon oxygenation, the bonding distances of the two axial histidines are shortened. Data obtained by Raman spectroscopy indicate that dioxygen is bound symmetrically; its binding involves an electron transfer process from both metal ions to the dioxygen molecule. The resulting site can actually be depicted as a peroxide adduct of a binuclear cupric complex (Freedman et al. 1976; Thamann et al. 1977). The reversibility of the oxygenation reaction is maintained by the high positive charge on the two metal centers and by the low dielectric constant of the surroundings of the metal binding site. Oxy-Hc is diamagnetic owing to the strong antiferromagnetic coupling of the unpaired spins of the two cupric centers. The estimate of coupling constants gives a value of 550–620 cm^{-1} (Solomon et al. 1975). Bound peroxide can be responsible for spin coupling in oxy-Hc. However, other bridging ligands may be involved: the presence of an ex-

* *Present address.* Albert Einstein College of Medicine, Yeshiva University, Bronx, NY 10461, USA

Correspondence to. L. Cordone

Abbreviations: Hc, Hemocyanin; M_0, zeroth moment; M_1, first moment, M_2, second moment; $(Co^{2+})_2$-Hc, binuclear bicobalt hemocyanin derivative; (Co^{2+})-Hc, mononuclear monocobalt hemocyanin derivative; $(Co^{2+}$-$Cu^{1+})$-Hc, binuclear mixed metals hemocyanin derivative; LFT, ligand field theory; CT, charge transfer; EPR, electronic paramagnetic resonance; XANES, X-ray absorption near edge structure

ogenous ligand X (e.g. H_2O or OH^-) bridging the two metal ions in the oxy form has been suggested (see e.g. Solomon 1981; Salvato and Beltramini 1990 and references therein). Actually this bridge is deemed necessary to account for the diamagnetism of met-Hc (Solomon 1981; Solomon et al. 1992).

The elucidation of the structure and of the properties of copper binding sites in proteins is the ultimate goal of the bioinorganic chemistry of this metal, since the variety of biological activities of copper proteins depends on a complex relationship linking the properties of the metal, the structure and organization of the binding site and the structure and dynamics of the protein matrix. In the case of Hcs, in spite of the great interest stimulated by their uncommon and striking properties, several aspects of the structure-function relationship remain to be solved.

The isomorphous substitution of the native metal with Co^{2+} proved to be a powerful tool for the understanding of the bioinorganic chemistry of copper sites. The similarity of the ionic radii of Cu^{2+} and Co^{2+}, together with the ability to give stables complexes with nitrogen ligands *via* unoccupied d-orbitals, allows one to obtain Co^{2+} derivatives specifically substituted at the copper sites. The advantage of such a substitution is that the optical and magnetic properties of the substituted derivative depend upon the geometry and immediate environment of the metal binding site. Among copper proteins, both mononuclear (carbonic anhydrase, azurin, plastocyanin, stellacyanin, type 1 laccase) (Coleman and Coleman 1972; McMillin et al. 1974a, b; Solomon et al. 1976; Larrabee and Spiro 1979) and binuclear (tyrosinase and hemocyanin) (Ruegg and Lerch 1981; Suzuki et al. 1985; Lorosch and Haase 1986; Salvato et al. 1986) proteins have been substituted. In apo-superoxide dismutase, the metal substitution can be directed specifically to the vacant copper or zinc site or to both sites (Salvato et al. 1989).

Optical spectroscopy over wide temperature ranges has proved to be a useful experimental tool in the study of structural and dynamic properties of the active site of metalloproteins (Cordone et al. 1986, 1988; Schomacker and Champion 1986; Srajer et al. 1986; Leone et al. 1987; Cupane et al. 1988, 1990). In fact, owing to the interaction of the optical electrons with the nearby nuclei, the optical absorption bands of a chromophore embedded in a matrix narrow and shift as the temperature is lowered. Moreover, in the case of charge-transfer bands, integrated intensity variations are also expected if, by lowering the temperature, variations in the overlap between the acceptor and donor orbitals occur (Cordone et al. 1986; Cupane et al. 1988). A rather simplified approach to the analysis of the temperature dependence of the optical spectra involves the calculation of the zeroth (M_0), first (M_1) and second (M_2) moments of a given absorption band (for definitions, see "Materials and methods"); within the harmonic Franck-Condon approximation it can be shown that the M_1 and M_2 temperature dependence can be approximated by the following expressions (Markham 1959; Baldini et al. 1965):

$$M_1 = D + F \coth(h\langle\nu\rangle/2\,\mathrm{kT}) \quad (1)$$

$$M_2 = A \coth(h\langle\nu\rangle/2\,\mathrm{kT}) + C^2$$

where $\langle\nu\rangle$ is the mean effective frequency of the nuclear motions coupled to the electronic transition and D, F, A and C are parameters linked to the Frank-Condon linear and quadratic coupling constants.

This approach does not give detailed information on the coupling constants of various Franck-Condon active vibrational modes with the electronic transition as well as on the various temperature independent line broadening mechanisms; rather it gives average information (mean effective frequency and coupling constants of the vibrational modes) on the dynamic properties of the matrix in the neighborhoud of the chromophore.

In the past few years the method described above has been successfully applied to study the dynamic properties of the active site of various metalloproteins, mainly ferrous derivatives of hemoglobin and myoglobin and the two blue copper proteins azurin and stellacyanin (Cordone et al. 1986; Leone et al. 1987; Cupane et al. 1988, 1990; Di Iorio et al. 1991).

In this work we have applied the above approach to analyze the temperature dependence of the optical absorption spectra of various cobalt-substituted derivatives of hemocyanin from *Carcinus maenas*. Three metal substituted protein derivatives have been studied; these are the binuclear $(Co^{2+})_2$ bi-substituted derivative, the mononuclear (Co^{2+}) derivative with only one cobalt ion in the "Cu_A" site and the binuclear mixed metal (Co^{2+}-Cu^{1+}) derivative (Bubacco et al. 1992). The aim of the study is to get insights into the stereodynamic properties of the active site and the eventual stabilizing effect of the metal ions.

Materials and methods

Hemocyanin from *Carcinus maenas* was purified as described by Beltramini et al. (1984). Substituted derivatives were prepared according to Bubacco et al. (1992). The concentration of both native, apo and Co^{2+} substituted protein was calculated from the absorbance at 278 nm using $\varepsilon_{278} = 1.24$ ml mg^{-1} cm^{-1}. Samples of Co^{2+}-Hc for spectrophotometric analysis were prepared in 20 mM potassium phosphate buffer pH 7.5 containing 65% (v/v) glycerol. In this solvent the sample remains transparent in the whole temperature range 300–20 K. Protein samples of approximatively 75–100 mg ml^{-1}, corresponding to 1.0–1.25 mM, were used. They were prepared by concentrating, by ultracentrifugation, the Co^{2+} protein derivative already dissolved in the glycerol containing buffer. A Spinco-Beckman Mod. L-2 ultracentrifuge and a 50TI rotor were used. The Co^{2+}-substituted proteins in buffer were split into portions and brought to 65% (v/v) glycerol. A first centrifugation was done at 48 000 rpm for 5 h. The supernatant was then discarded and the concentrated samples were pooled and centrifuged again at 46 000 rpm for 7 h. Under these conditions, the protein is sharply concentrated at the bottom of ultracentrifuge tube and the sample, after discarding the excess solvent, is stored at −20 °C until used. The aggregation state of our samples has been reported to be mainly hexameric at room temperature (16 S sedimentation coefficient; Salva-

to and Beltramini 1990). The freezing procedure can be harmful for Hc unless the solution contains either sucrose or glycerol. The latter compound is used in the present work both to obtain a good quality glass and to prevent aggregation state variations at low temperatures. In fact, EPR spectra at 4 K indicate the presence of high spin Co^{2+} with no indication for damaged sites; moreover, optical spectra show no variation of light scattering with temperature, that are expected in the case of extensive dissociation (see Figs. 1, 4 and 6).

The experimental setup and methods for optical measurements in the temperature range 300–20 K have been described previously (Cordone et al. 1986). Spectra (650–470 nm) were taken with a Jasco Uvidec 650 spectrophotometer (bandwidth = 0.4 nm; time constant = 1 s; scan speed = 40 nm/min). The baseline (cuvette + solvent + buffer) measured at room temperature was subtracted from each spectrum, since in the spectral region of interest the baseline does not depend on temperature. Spectral data were recorded at 0.8 nm intervals. Deconvolution of the spectra into Gaussian components was performed according to

$$A(\nu)=\sum_{i=1}^{N} I_i \exp[-(\nu-\nu_{0i})^2/2\sigma_i^2]$$

where $A(\nu)$ is the absorbance at frequency ν, I_i, ν_{0i}, σ_i are the amplitude, peak position and halfwidth of the i-th component and N is the number of components. An HP-1000 computer was used and the mean square deviation was minimized using a non linear least-squares algorithm (Marquardt 1963). Errors on fitted parameters were calculated by inversion of the curvature matrix, within the approximation of parabolic χ^2 surface around the minimum; they correspond to 67% confidence limits. Within the so called narrow band approximation (Dexter 1958) the zeroth (M_0), first (M_1) and second (M_2) moments of a band are defined as:

$$M_0=\int_0^\infty A(\nu)\,d\nu$$

$$M_1=M_0^{-1}\int_0^\infty \nu A(\nu)\,d\nu$$

$$M_2=M_0^{-1}\int_0^\infty \nu^2 A(\nu)\,d\nu-M_1^2 .$$

In the present case of Gaussian bands $M_{0i}=\sqrt{2\pi}\,I_i\,\sigma_i$; $M_{1i}=\nu_{0i}$; $M_{2i}=\sigma_i^2$.

Results and discussion

a) Binuclear bicobalt derivative [$(Co^{2+})_2$–Hc]

Figure 1 (left panel) shows the optical absorption spectra of $(Co^{2+})_2$-Hc at various temperatures. In the low temperature spectra three peaks are clearly resolved; no vibronic structure, however, is detected. The presence of three different bands that partially overlap and the absence of a vibronic structure does not enable us to perform the analysis of the spectra in terms of vibrationally coupled bands (Srajer et al. 1986; Mantini et al. 1989; Di Pace et al. 1992; Leone et al. 1992); we have therefore deconvoluted the measured spectra in terms of Gaussian components. The deconvolution of the 20 K spectrum is shown in Fig. 1, right panel. As can be seen, fittings with three Gaussian bands (denoted A, B and C in order of increasing peak frequency) are satisfactory; a fourth Gaussian component centered at 20 000 cm^{-1} is added as an extrapolation to take into account the background generated by higher frequency transitions and from scattered light.

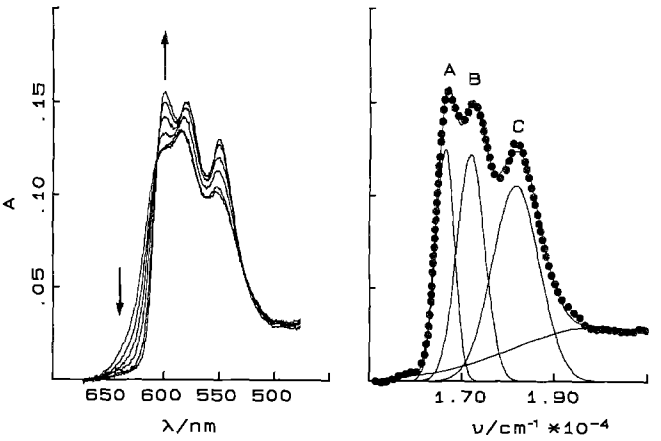

Fig. 1. *Left panel:* optical absorption spectra of $(Co^{2+})_2$–Hc at T = 290, 240, 190, 130, 80 and 20 K. The arrows at about 630 and 660 nm indicate the direction of spectral changes observed on lowering the temperature. *Right panel.* deconvolution of the 20 K absorption spectrum of $(Co^{2+})_2$–Hc in terms of Gaussian components. •: experimental points; continuous lines represent the Gaussian components and the synthesized band profile. For the sake of clarity, not all the experimental points have been reported. The root mean square deviation (expressed in A units) is 2×10^{-3}

The temperature dependence of M_0, M_1 and M_2 relative to the three bands observed is reported in Figs. 2 (left panel) and 3. The continuous lines in Fig. 3 represent fittings of M_1 and M_2 in terms of Eqs. (1); values of the relevant parameters obtained from the fittings are reported in Table 1. Data in left panel of Fig. 2 show that by lowering the temperature bands A and B displays large intensity variations whereas the intensity of band C remains almost unchanged. Temperature induced intensity variations can be interpreted, for metal ↔ ligand charge transfer bands, in terms of alteration in the relative positions of metal and ligand that, in turn, cause alterations in the overlap between the orbitals involved in the electronic transition (Cordone et al. 1986; Cupane et al. 1988, 1990) or in terms of thermally populated d-orbital electronic states (Srajer and Champion 1991). Such mechanisms are clearly not operative for pure π-π^* or d-d transitions. In view of their large intensity variations with temperature, bands A and B should therefore arise either from charge transfer transitions or at least from transitions having partial charge-transfer character; we also tentatively attribute band C, whose intensity is almost temperature independent, to a cobalt d-d transition.

Concerning the M_1 and M_2 temperature dependence (data shown in Fig. 3 and in Table 1), we note that rather satisfactory fittings are obtained by using Eq. (1); this indicates that the simplified moment analysis described in

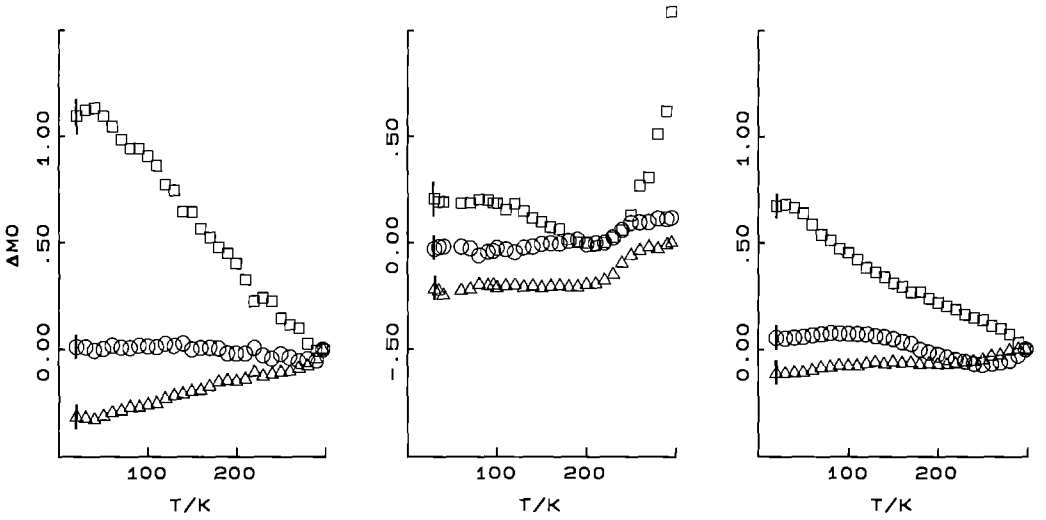

Fig. 2. ΔM_0 relative to the optical absorption bands of the Hc derivatives studied as a function of temperature. *Left panel*: $(Co^{2+})_2$–Hc; *middle panel*: (Co^{2+})–Hc; *right panel*. $(Co^{2+}$–$Cu^{1+})$–Hc. △: band A; □: band B; ○: band C. Typical error bars are shown. ΔM_0 is defined as $M_0(T)/M_0(290\ K) - 1$. In view of the non regular behaviour of bands B and C of (Co^{2+})–Hc at temperatures higher than 210 K (see also Fig. 5 and discussion in the text) M_0 values relative to these bands have been normalized at 210 K

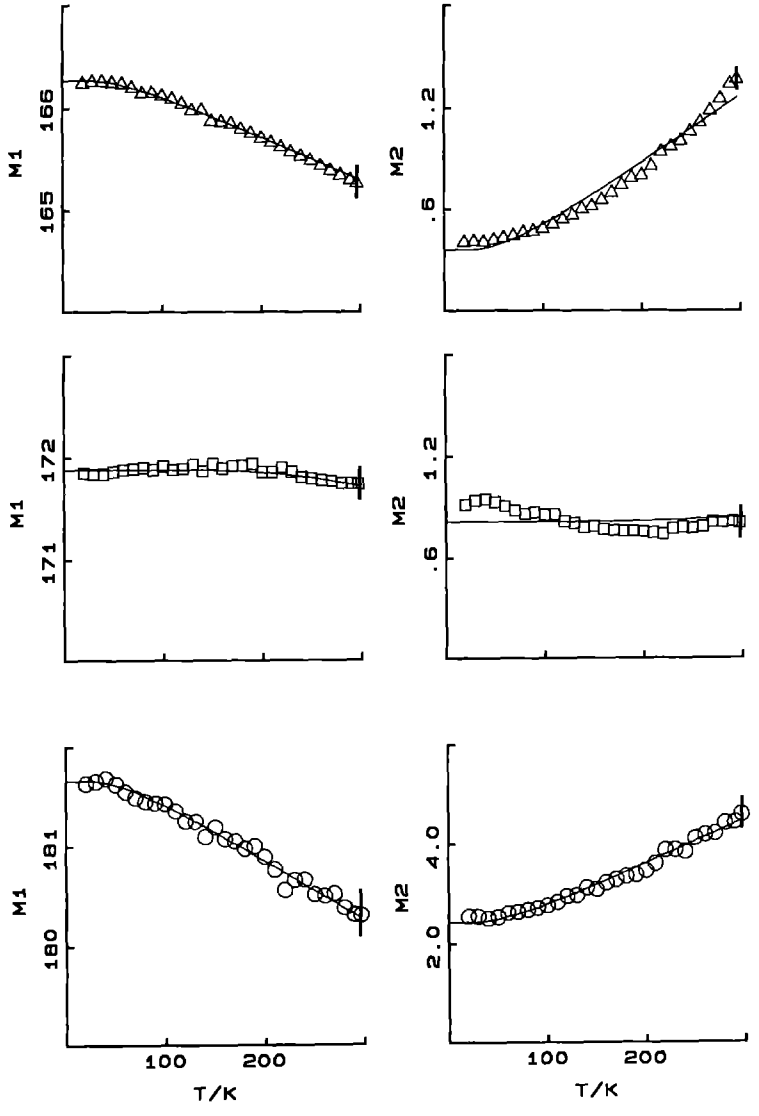

Fig. 3. M_1 (*left*) and M_2 (*right*) relative to the optical absorption bands of $(Co^{2+})_2$–Hc. Symbols as in Fig. 2. Continuous lines represent the best fit of eq. (1) to the experimental points. The M_1 scale is in units of $10^{-2} \times cm^{-1}$; the M_2 scale is $10^{-5} \times cm^{-2}$. Error bars at high temperature are shown; due to the increased spectral resolution, errors decrease as the temperature decreases

Table 1. Electron-vibration mean effective coupling parameters of $(Co^{2+})_2$-Hc. Values of parameters were obtained by fitting the M_1 and M_2 thermal behavior in terms of Eq. (1)

Band	ν (cm^{-1})	A ($10^{-4} \times cm^{-2}$)	C (cm^{-1})	F (cm^{-1})	D (cm^{-1})
A	140± 20	3.7±0.2	0±10	− 48± 10	16,674± 4
B	≥800	5 ±1[a]	178±100[a]	−277±100[a]	17,466±127[a]
C	140± 20	9.6±1	391±17	− 64± 13	18,255± 4

[a] The rather large errors in the parameters for band B is due to the fact that, for this band, M_1 and M_2 are almost temperature indepedendent

the introduction can reasonably be applied to our data. In Fig. 3, systematic misfits with respect to the behavior predicted by Eq. (1) are evident particularly for the second moment of band A. Such misfits suggest the presence of non-harmonic contributions to the soft modes coupled with the chromophore (Di Pace et al. 1992; Cupane et al. 1993); however, due to the "heuristic" spectral deconvolution used in this work that does not enable us to single out the various contributions to the linewidth, we prefer to neglect such contributions and therefore consider the bi-cobalt derivative as "essentially harmonic".

Band A exhibits a marked M_1 and M_2 temperature dependence that is indicative of its coupling to low frequency vibrational modes whose mean effective frequency is about 140 cm^{-1}. In the resonance Raman spectra of blue copper proteins (Ferris et al. 1979; Nestor et al. 1984; Woodruff et al. 1984) several peaks are found at 140–160 cm^{-1} and are attributed to ligand-metal-ligand deformation modes (Woodruff et al. 1984). In view of this finding we propose that band A should be assigned to an electronic transition having substantial admixture with a $\pi_{NHis} \rightarrow d_{Co}$ transition. In contrast, M_1 and M_2 relative to band B are almost temperature independent; this indicates coupling to high frequency modes whose mean effective frequency is higher than 800 cm^{-1}. We suggest that band B should be assigned to an electronic transition having substantial admixture with a $\pi_X \rightarrow d_{Co}$ charge transfer transition, i.e. with a transition from the π orbitals of the exogenous bridging ligand into the cobalt d orbitals. The vibrational modes coupled to this transition are probably Co–ligand–Co stretching or bending modes and their high frequency suggests that the exogenous ligand is rather strongly bound to the two metal ions.

M_1 and M_2 relative to band C again exhibit a marked temperature dependence indicative of the coupling of this band to low frequency ($\langle\nu\rangle \approx 140$ cm^{-1}) vibrational modes. Band C has already been assigned to a cobalt d-d transition; data in Fig. 3 and in Table 1 therefore suggest that the cobalt d orbitals involved are coupled to the N_{His}–Co–N_{His} deformation modes mentioned above.

The above suggested assignments for bands A and B deserve some comment.

Optical spectra of several Co^{2+}-containing chromophores have been studied previously; these include cobalt substituted blue copper proteins (McMillin et al. 1974a, b; Solomon et al. 1976), cobalt substituted carbonic anhydrase (Coleman and Coleman 1972), model systems involving Co^{2+} complexes with 2,2′-Bis(2-imidazolyl)biphenyl (Knapp et al. 1990), the binuclear centers in cobalt tyrosinase (Ruegg and Lerch 1981) and in cobalt hemocyanin (Lorosch and Haase 1986). In all these systems from two to four bands, more or less resolved, are observed in the wavelength region 650–500 nm; moreover the intensity of the bands suggests that, in these chromophores, the Co^{2+} ion is in pseudo-tetrahedral coordination. For a d^7 ion in tetrahedral symmetry the ligand field theory (LFT) predicts three spin allowed d-d transitions: $^4A_2 \rightarrow {}^4T_2$, $^4A_2 \rightarrow {}^4T_1(F)$, $^4A_2 \rightarrow {}^4T_1(P)$. By taking the values of 5 000 cm^{-1} for tetrahedral field strength and of 800 cm^{-1} for the Racah B parameter (Griffith 1961), one obtains ν_1 ($^4A_2 \rightarrow {}^4T_2$)$\approx$ 5 000 cm^{-1}; ν_2 ($^4A_2 \rightarrow {}^4T_1(F)$)$\approx$9 000 cm^{-1}; ν_3 ($^4A_2 \rightarrow {}^4T_1(P)$)$\approx$18 000 cm^{-1}; therefore a single d-d band is expected in the frequency range relevant to this paper. The splitting between the observed bands ($\approx$1 000 cm^{-1}) is too large to be attributed to spin-orbit coupling effects (whose strength is $\approx$150 cm^{-1} (Lever 1984)); for this reason the presence of several bands in the visible region is usually attributed to splitting of the $^4A_2 \rightarrow {}^4T_1(P)$ d-d transition due to distortions from tetrahedral symmetry. It has also to be mentioned that, at sufficiently high values of the crystal field strength, some doublet states may lie at energies near to that of the $^4T_1(F)$ level (Weakliem 1962); the presence of other spin-forbidden d-d transitions in the visible region cannot therefore be excluded.

As far as the charge transfer (CT) transitions are concerned, the $\pi_{NHis} \rightarrow d_{Cu}$ transition has been observed at about 20 000 cm^{-1} in blue copper proteins (Solomon et al. 1980). In view of the smaller electron affinity of Co^{2+} with respect to Cu^{2+}, the $\pi_{NHis} \rightarrow d_{Co}$ charge transfer transition is expected at higher frequency in the cobalt chromophore and, indeed, charge transfer bands (attributed to $\pi_{NHis} \rightarrow d_{Co}$ transitions) have been observed at about 32 000 cm^{-1} in cobalt substituted blue copper proteins (McMillin et al. 1974a, b; Solomon et al. 1976) and in tetrahedral Co^{2+} complexes having imidazole ligands (Knapp et al. 1990). These data seem to exclude the presence of a $\pi_{NHis} \rightarrow d_{Co}$ transition in the visible region; since the "intensity stealing" phenomenon is inversely related to the energy separation between the transitions concerned, the mechanism proposed above to account for the temperature dependence of M_0, M_1 and M_2 relative to band A could seem unlikely. It must be noted, however, that in all the above mentioned Co^{2+} containing chromophores, all the N_{His}–Co distances are reported to be about 1.9 Å. The frequency of a CT transition can be written as $h\nu_{CT} = I_D - E_A + \Delta$ where I_D is the ionization potential of the donor, E_A is the electron affinity of the acceptor and Δ is a term arising from the electrostatic interaction of the acceptor-donor system (other terms arising from exchange interactions can be usually neglected). Since in the excited state N^+ and Co^+ repel each other the term Δ contributes a positive term to $h\nu_{CT}$ that is a decreasing function of the N–Co distance. An approximate calculation of Coulomb repulsion between unitary electronic point charges at 1.9 Å distance leads to $d\Delta/dR = -3.3$ eV/Å; an increase of the N–Co distance from 1.9 to 2.2 Å should therefore cause a ν_{CT} redshift of

about 14 000 cm^{-1}. The presence of a $\pi_{NHis} \rightarrow d_{Co}$ CT transition in the visible range seems therefore to us, in the case of cobalt-substituted Hc, not unrealistic.

Further evidence for the involvement of CT transition in the visible absorption spectra of cobalt-substituted Hc comes from the thermal behavior of the 350 nm and 570 nm absorption bands of copper oxyhemocyanin. In fact, both these bands have been attributed to $O_2^{2-} \rightarrow Cu^{2+}$ CT transitions (Himmelwright et al. 1980; Loehr et al. 1974; Freedman et al. 1976); recent experiments at our laboratory on the temperature dependence of these bands (unpublished results) have shown that, for both bands, large integrated intensity variations occur as the temperature is lowered.

In conclusion, the data reported do not enable us to unambiguously assign bands A and B. However, the temperature dependence of their zeroth, first and second moments does suggest that the electronic transitions responsible for these bands (that could also involve e.g. splitting components of the $^4A_2 \rightarrow {}^4T_1$ (*P*) transition or spin forbidden *d-d* transitions to doublet states) are mixed with charge transfer states and that the π orbitals of the ligands N_{His} and X (possibly OH^-) are involved. This fact would explain both the large temperature induced intensity variations and the coupling of the bands with the $N_{His}-Co-N_{His}$ (band A) and the X–Co (band B) vibrations.

It should also be mentioned that recent molecular orbital calculations (performed on the $[(NH_3)_3-Cu]_2^{4+}$ model system) point out that the higher lying frontier orbitals of this system are mainly made of Cu *d* orbitals but have substantial admixture with NH_3 lone pairs (Kitajima et al. 1992).

From the reported results we derive a description of the active site of $(Co^{2+})_2$–Hc as a rather homogeneous and symmetric site in which the two cobalt ions occupy spectroscopically equivalent positions (as suggested by the fact that only three bands are observed even at 20 K) and whose dynamics, within the limits of the analysis adopted, is characterized up to room temperature by "essentially harmonic" vibrations. Moreover, data relative to band B provide evidence in favour of the presence, in the active site, of an exogenous bridging ligand that is rather strongly bound by the two cobalt ions. The presence of an exogenous bridging ligand in cobalt Hc derivatives was also recently suggested by EPR studies (Bubacco et al. 1992), where an H_2O molecule or an OH^- ion was proposed to be responsible for strong coupling between the two cobalt ions. Furthermore, XANES investigations on the same derivative (Della Longa et al., private communication) point out the presence of an exogenous ligand to account for the experimentally observed nearly tetrahedral coordination of each metal ion. In our opinion the fact that the X-ray structure of copper deoxy-Hc shows no evidence for an exogenous ligand with 7 Å from the copper ions does not contradict the present suggestion, owing to the limited resolution of the X-ray structure (Volbeda and Hol 1989) and also to the different charges of the metal ions.

b) Mononuclear monocobalt derivative [(Co^{2+})–Hc]

Figure 4 shows the spectra of (Co^{2+})–Hc in the temperature ranges of 20–210 K (left panel) and of 210–295 K (middle panel). As can be seen the thermal behavior of the raw spectra is almost regular from 20 to 210 K and changes drastically at higher temperatures. At low temperatures three bands are again clearly identified, although the three peaks are blue shifted with respect to those of $(Co^{2+})_2$–Hc. The shoulder that appears on the low frequency side is at exactly the same frequency as band A relative to $(Co^{2+})_2$–Hc; we therefore attribute this shoulder to the presence of a small fraction of protein with two cobalt ions in the active site. In view of its smallness, however, the shoulder has been neglected in the spectral analysis. The deconvolution of the 20 K spectrum is also shown in Fig. 4 (right panel). Again, fittings

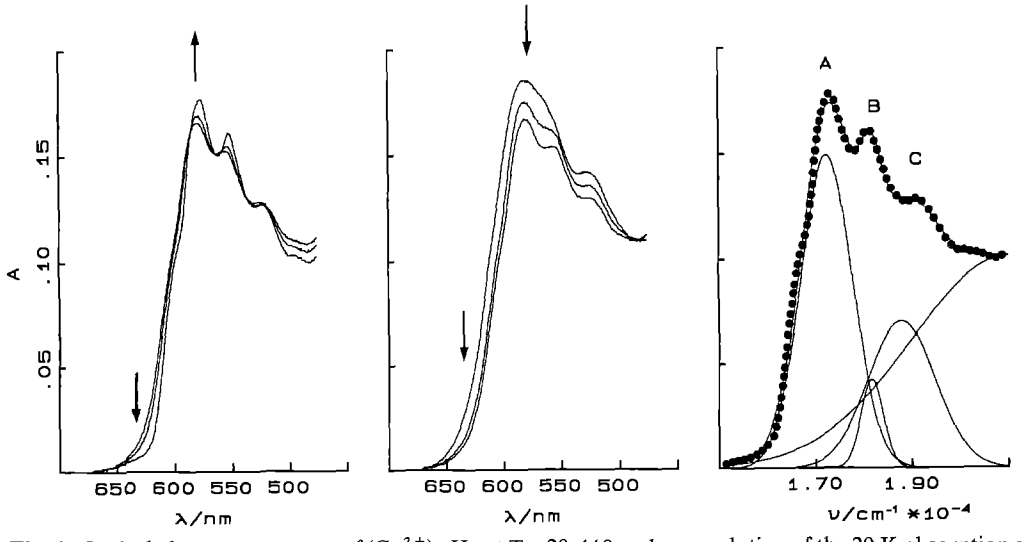

Fig. 4. Optical absorption spectra of (Co^{2+})–Hc at T = 20, 110 and 200 K (*left panel*) and T = 220, 250 and 290 K (*center panel*). The arrows at about 630 and 600 nm indicate the direction of spectral changes observed on lowering the temperature. *Right panel:* deconvolution of the 20 K absorption spectrum of (Co^{2+})–Hc in terms of gaussian components. Symbols as in the right panel of Fig. 1. The root mean square deviation (expressed in A units) is 2×10^{-3}

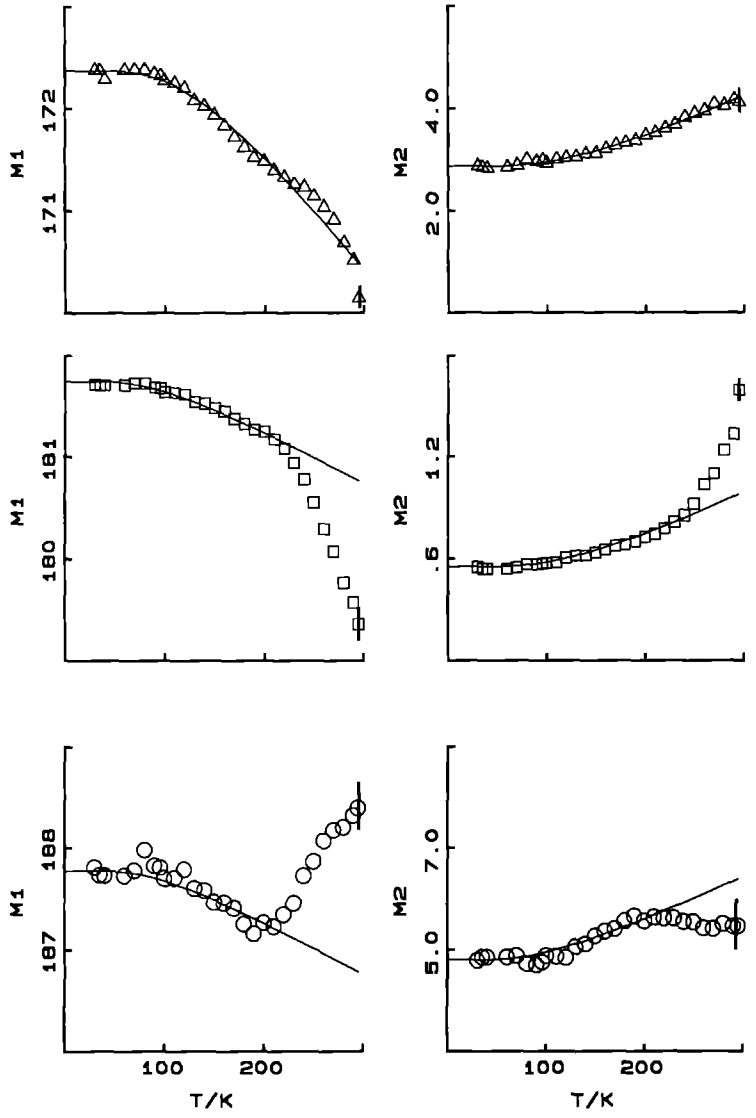

Fig. 5. M_1 (*left*) and M_2 (*right*) relative to the optical absorption bands of (Co^{2+})–Hc. Symbols as in Fig. 2. Continuous lines represent the best fit of Eq. (1) to the experimental points in the temperature range of 20–210 K. The M_1 scale is in units of $10^{-2} \times cm^{-1}$; the M_2 scale is $10^{-5} \times cm^{-2}$. *Error bars* as in Fig. 3

with three Gaussian bands (denoted A, B and C in order of increasing peak frequency) are satisfactory. A fourth Gaussian component centered at 20 000 cm^{-1} is added as an extrapolation to take into account the background generated by higher frequency transitions and from scattered light. It should be noted that the intensity of this extrapolation is much higher for (Co^{2+})–Hc than for $(Co^{2+})_2$–Hc. We attribute this fact to the increased light scattering (indeed, higher protein concentrations are needed to obtain good spectra, in view of the lower extinction coefficient of the monocobalt derivative); we stress that the results obtained are independent on the kind of extrapolation used and that essentially identical results are obtained by using a tangent straight line or even a $1/\lambda^4$ type extrapolation.

The M_0 temperature dependence (reported in the middle panel of Fig. 2) suggests for bands A, B and C the same assignment as suggested for the analogous bands relative to the binuclear bicobalt derivative; indeed, large M_0 variations are observed for bands A and B, whereas the integrated intensity of band C is scarcely influenced by temperature.

The M_1 and M_2 thermal behavior is shown in Fig. 5. In agreement with what has been noted from the inspection of the raw spectra, Eq. (1) cannot be fit to the data in the whole temperature range, particularly for bands B and C; a fitting of the same quality as for the binuclear derivative can be performed in the range 20–210 K. The continuous lines in Fig. 5 represent such fittings; values of the relevant parameters are reported in Table 2.

In analogy with the binuclear $(Co^{2+})_2$ derivative, bands A and C are coupled to low frequency vibrations (although the values of the mean effective frequencies are slightly larger than those for the bi-cobalt derivative). A marked difference between the two derivatives is evident for band B; in fact, the mean effective frequency of nuclear vibrations coupled to this band is greater than 800 cm^{-1} for $(Co^{2+})_2$–Hc and only 270 cm^{-1} for the monocobalt derivative. This result, consistent with the presence of the above mentioned exogeneous ligand X and with the attribution of band B to an electronic transition having a substantial admixture with a $\pi_X \rightarrow d_{Co}$ charge transfer transition, indicates that in the presence of only one metal ion in the active site the exogenous

ligand is less tightly bound and that the X–Co stretches occur at a much lower frequency.

From Fig. 5 it is also evident that very large deviations from the behavior predicted by Eq. (1) occur, both for M_1 and M_2 of bands B and C, at temperatures higher than 210 K. The same effect also seems to be present, although to a much lesser extent, for band A.

We attribute these deviations to the onset of disordered motions that involve the exogenous ligand X and, quite likely, the entire active site; they are greatly hindered in the binuclear bicobalt derivative since the presence of the second metal ion stabilizes the bridging ligand X and the overall structure of the active site.

Three further features of the data in Tables 1 and 2 are worth noting:

1) parameter C seems to be larger for the monocobalt than for the bicobalt derivative. This agrees with a greater conformational heterogeneity at low temperatures of (Co^{2+})–Hc with respect to $(Co^{2+})_2$–Hc; this interesting conclusion, however, cannot be unambiguously claimed since the various line broadening mechanisms contributing to the C value are not resolved in the present kind of spectral analysis;

2) parameter $\langle \nu \rangle$ relative to bands A and C seems to be larger for the monocobalt ($220 \div 270\ cm^{-1}$) than for the bicobalt derivative ($140\ cm^{-1}$). This could be explained by suggesting that in the mononuclear derivative, owing to the absence of the second metal ion, the Co–N distances are slightly shorter than in the binuclear derivatives making force constants and therefore the frequencies of the N–Co–N deformation modes higher. This suggestion would be consistent with the diminished reactivity of the Co^{2+} in the "Cu_A" site; a direct confirmation, however, could be obtained with X-ray crystal diffraction or, in solution, with resonance Raman spectroscopy;

3) values of the peak frequencies of the three bands (or, equivalently, of the parameter D in Tables 1 and 2), appear to be systematically higher for the monocobalt than for the bicobalt derivative. This can be explained with a simple electrostatic argument by considering the stabilizing effect of the positive charge of the second cobalt ion on the *d* orbitals of the first cobalt ion involved in the electronic transitions, and supports the suggested correspondence of bands A, B and C in the mononuclear derivative to the analogous ones in the binuclear derivative.

From the reported results we derive a description of the active site of (Co^{2+})–Hc as a rather heterogeneous site whose dynamics are characterized, in the range 20–210 K, by essentially harmonic vibrations and at higher temperatures, by disordered motions. These motions obviously involve the exogenous ligand that, at temperatures higher than 210 K, undergoes highly disordered motion.

c) Binuclear mixed metals derivative $[(Co^{2+}-Cu^{1+})-Hc]$

Figure 6 (left panel) shows the spectra of $(Co^{2+}-Cu^{1+})$–Hc at various temperatures. The low temperature spectra

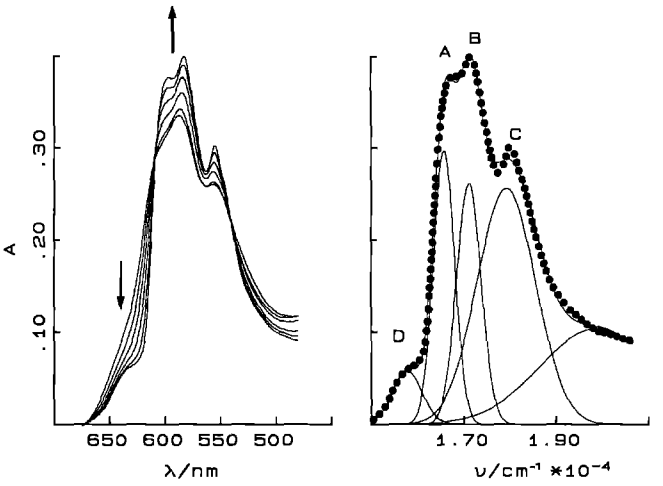

Fig. 6. *Left panel:* optical absorption spectra of $(Co^{2+}-Cu^{1+})$–Hc at T = 290, 240, 190, 130, 80 and 20 K. The arrows at about 630 and 600 nm indicate the direction of spectral changes observed on lowering the temperature. *Right panel:* deconvolution of the 20 K absorption spectrum of $(Co^{2+}-Cu^{1+})$–Hc in terms of gaussian components. Symbols as in the right panel of Fig. 1. The root mean square deviation (expressed in A units) is 5×10^{-3}

Table 2. Electron vibration mean effective coupling parameters of (Co^{2+})–Hc. Parameters values were obtained by fitting the M_1 nd M_2 thermal behavior, in the temperature range 20–210 K, in terms of Eq. (1)

Band	ν (cm^{-1})	A ($10^{-4} \times cm^{-2}$)	C (cm^{-1})	F (cm^{-1})	D (cm^{-1})
A	270±20	18 ±2.3	327± 33	−271±57	17,508±20
B	270±30	5.5±2	122± 50	− 78±20	18,228± 7
C	220±50	13.4±5	588±100	− 82±20	18,860±50

are more complex than those of $(Co^{2+})_2$–Hc and, besides three well resolved peaks, a small band appears in the low frequency wing. The increased complexity of the spectra is to be expected, in view of the non symmetric active site of this derivative. We tentatively assign the low frequency band to a *d-d* transition of Cu^{2+} traces likely arising from an oxidative side reaction. The smallness of the band, however, does not enable us to obtain relevant information from its temperature dependence. The deconvolution of the 20 K spectrum is shown in the right panel of Fig. 6. As can be seen, fittings with four Gaussian bands (the three main bands are denoted, as usual, A, B and C in order of increasing frequency, whereas the small low frequency band is denoted as D) are satisfactory; as usual, a further Gaussian component centered at 20 000 cm^{-1} is added as an extrapolation. The temperature dependence of M_0, M_1 and M_2 relative to the three main bands are reported in the right panel of Fig. 2 and in Fig. 7. The continuous lines in Fig. 7 represent fittings of M_1 and M_2 in terms of Eq. (1); values of the relevant parameters are reported in Table 3. In analogy with the bicobalt derivative, the quality of the fittings (particularly for the second moment of band A) is such that the presence of small non harmonic contributions to the soft modes coupled with

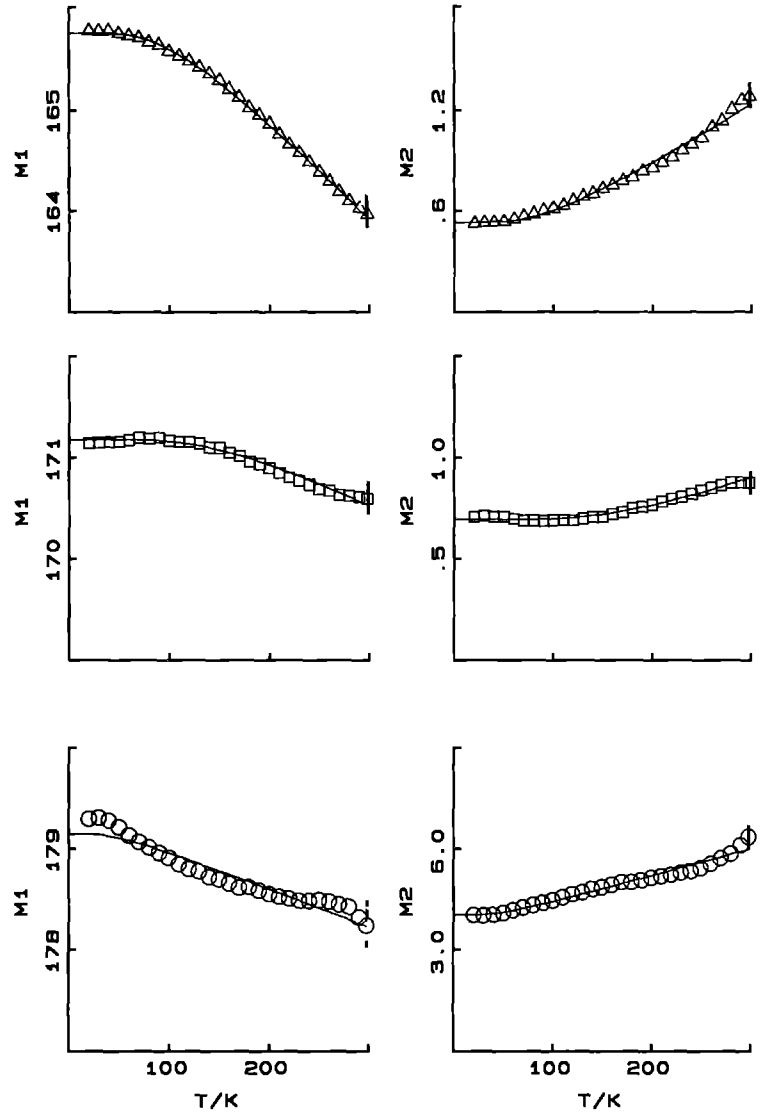

Fig. 7. M_1 (*left*) and M_2 (*right*) relative to the optical absorption bands of $(Co^{2+}-Cu^{1+})$–Hc. Symbols as in Fig. 2. Continuous lines represent the best fit of Eq. (1) to the experimental points. The M_1 scale is in units of $10^{-2} \times cm^{-1}$; the M_2 scale is $10^{-5} \times cm^{-2}$. *Error bars* as in Fig. 3

the chromophore cannot be excluded. Once more, the kind of spectral deconvolution adopted does not enable to discuss such terms and therefore the mixed metal Hc derivative is considered as "essentially harmonic".

Data in Figs. 2 and 7 and in Table 3 are fully consistent with the suggestions drawn from analogous data for bicobalt and monocobalt Hc derivatives and in particular:

i) bands A and B display large M_0 variations with temperature while the integrated intensity of band C is almost temperature independent.

ii) bands A and C are coupled to low frequency modes and, in analogy with $(Co^{2+})_2$–Hc, mean effective frequency values of about 140 cm^{-1} are observed. Band B is coupled to higher frequency modes, confirming that in binuclear derivatives the exogenous ligand X is tightly bound; the mean effective frequency value (410 cm^{-1}) is, however, lower than for the fully symmetric bicobalt derivative.

iii) values of parameter C are smaller than those for the monocobalt Hc derivative; moreover, peak frequency values for the three bands are very similar to those for $(Co^{2+})_2$–Hc, as expected from the simple electrostatic argument outlined above.

Table 3. Electron-vibration mean coupling parameters of $(Co^{2+}-Cu1^{+})$–Hc. Parameters values were obtained by fitting the M_1 and M_2 thermal behaviour in terms of Eq. (1)

Band	ν (cm^{-1})	A ($10^{-4} \times cm^{-2}$)	C (cm^{-1})	F (cm^{-1})	D (cm^{-1})
A	190±20	5.3±0.1	0±10	−164±10	16,739± 4
B	410±40	6 ±1	97±50	−140±27	17,258±10
C	120±40	5.3±2	591±20	− 25±10	17,940± 8

From the reported results we derive a description of the active site of $(Co^{2+}-Cu^{1+})$–Hc as a rather homogeneous but non symmetric site whose dynamics are characterized up to room temperature by "essentially harmonic" vibrations. The exogenous ligand is rather strongly bound to the two metal ions although less strongly than in the symmetric bicobalt Hc derivative.

Conclusions

The analysis of the thermal behavior of the spectra of the three Hc derivatives studied has enabled to suggest that ligand to metal charge transfer transitions contribute to the intensity of the visible absorption bands. Moreover, the analysis of the temperature dependence of the first and second moment of the bands has provided information on the stereodynamic properties of the active site of Hc. In binuclear Hc derivatives the active site appears to be characterized by essentially harmonic vibrational motions (within the limits of our analysis) and the exogenous ligand X is strongly bound to the two metal ions. In the mononuclear Hc derivative the active site appears to be characterized by harmonic vibrational motion only in the temperature range 20–210 K, although the exogeneous ligand is much less tightly bound than in binuclear derivatives. At temperatures higher than 210 K the onset of disordered motions that involve the exogenous ligand and, quite likely, the entire active site are evident. This kind of motions is greatly hindered in the binuclear derivatives, owing to the marked stabilizing effect of the second metal ion not only on the exogenous ligand but also on the overall structure of the active site.

Acknowledgements. The authors are indebted to Prof. A. Bianconi and Dr. S. Della Longa for useful discussions and to Mr. G. Lapsis and Mr. M. Quartararo for their skilful technical help. This work has been supported by grants from MURST and from CNR. General indirect from CRRNSM is also gratefully acknowledged.

References

Baldini G, Mulazzi E, Terzi N (1965) Isotope effects induced by local modes in the U band. Phys Rev A140:2094–2101

Beltramini M, Ricchelli F, Tallandini L, Salvato B (1984) The reaction between cyanide and hemocyanin of *Carcinus maenas*. A kinetic study. Inorg Chim Acta 92:219–227

Bubacco L, Magliozzo RS, Beltramini M, Salvato B, Peisach J (1992) Preparation and spectroscopic characterization of a coupled binuclear center in Co(II)-substituted hemocyanin. Biochemistry 31:9294–9303

Coleman JE, Coleman RV (1972) Magnetic circular dichroism of Co(II) Carbonic Anhydrase. J Biol Chem 247:4718–4728

Cordone L, Cupane A, Leone M, Vitrano E (1986) Optical absorption spectra of deoxy- and oxyhemoglobin in the temperature range 300–20 K: relation with protein dynamics. Biophys Chem 24:259–275

Cordone L, Cupane A, Leone M, Vitrano E, Bulone D (1988) Interaction between external medium and haem pocket in myoglobin probed by low-temperature optical spectroscopy. J Mol Biol 198:213–218

Cupane A, Leone M, Vitrano E, Cordone L (1988) Structural and dynamic properties of the heme pocket in myoglobin by optical spectroscopy. Biopolymers 27:1977–1997

Cupane A, Leone M, Vitrano E, Cordone L (1990) Optical absorption spectra of azurin and stellacyanin in glicerol/water and ethylene glycol/water solutions in the temperature range 290–20 K. Biophys Chem 38:213–224

Dexter DL (1958) In: Seitz F, Turnbull D (eds) Solid state physics. Academic Press, New York

Di Iorio EE, Hiltpold UR, Filipovic D, Winterhalter KH, Gratton E, Vitrano E, Cupane A, Leone M, Cordone L (1991) Protein dynamics: Comparative investigation on heme-proteins with different physiological roles. Biophys J 59:742–754

Di Pace A, Cupane A, Leone M, Vitrano E, Cordone L (1992) Vibrational coupling, spectral broadening mechanisms and anharmonicity effects in carbonmonoxy heme proteins studied by the temperature dependence of the Soret band lineshape. Biophys J 63:475–484

Ferris NS, Woodruff WH, Tennent DL, McMillin DR (1979) Native azurin and its Ni(II) derivative: a resonance Raman study. Biochem Biophys Res Commun 88:288–296

Freedman TB, Loehr JS, Loehr TM (1976) A resonance Raman study of the copper protein Hemocyanin. New evidence for the structure of the oxygen binding site. J Am Chem Soc 98:2809–2815

Gaykema WPJ, Hol WGJ, Vereijken JM, Soeter NM, Bak HJ, Beintema JJ (1984) 3.2 Å structure of the copper containing, oxygen carrying protein *Panulirus interruptus* haemocyanin. Nature 309:23–29

Griffith JS (1961) The theory of transition-metal ions. Cambridge University Press, Cambridge

Himmelwright RS, Eickman NC, LuBien CD, Solomon EI (1980) Chemical and spectroscopic comparison of the binuclear copper active site of mollusc and arthropod hemocyanins. J Am Chem Soc 102:5378–5388

Hol WGJ, Volbeda A, Hazes B (1990) Structural studies of *Panulirus interruptus* hemocyanin. In: Preaux G, Lontie R (eds) Invertebrate dioxygen carriers. Leuvain University Press, pp 185–188

Kitajima N, Fujisawa K, Fujimoto C, Morooka Y, Hashimoto S, Kitagawa T, Toriumi K, Nakamura A (1992) A new model for dioxygen binding in Hemocyanin. Synthesis, characterization and molecular structure of the peroxo dinuclear copper (II) complexes, $[Cu(HB(3,5\text{-}R_2pz)_3]_2(O_2)$ (R = i-Pr and Ph). J Am Chem Soc 114:1277–1291

Knapp S, Keenan TP, Zhang X, Fikar R, Potenza JA, Schugar HJ (1990) Preparation, structure and properties of pseudotetrahedral D_{3d} complexes of Cu(II), Ni(II), Co(II), Cu(I) and Zn(II) with the geometrically constraining bidentate ligand 2,2′-Bis(2-imidazolyl)biphenyl. Examination of electron self-exchange for the Cu(I)/Cu(II) pair. J Am Chem Soc 112:3452–3464

Larrabee JA, Spiro TG (1979) Cobalt II substitution in the type I site of the multicopper oxidase rhus laccase. Biochem Biophys Res Commun 88:753–760

Leone M, Cupane A, Vitrano E, Cordone L (1987) Dynamic properties of oxy- and carbonmonoxyhemoglobin probed by optical spectroscopy in the temperature range 300–20 K. Biopolymers 26:1769–1779

Leone M, Cupane A, Vitrano E, Cordone L (1992) Strong vibronic coupling in heme proteins. Biophys Chem 42:111–115

Lever ABP (1984) Inorganic electronic spectroscopy. Elsevier, Amsterdam

Loehr JS, Freedman TB, Loehr TM (1974) Oxygen binding to Hemocyanin: a resonance Raman spectroscopic study. Biochem Biophys Res Commun 56:510–515

Lorosch J, Haase W (1986) Cobalt (II)-Hemocyanin: a model for the cuprous deoxy protein given evidence for a bridging ligand in the active site. Biochemistry 25:5850–5857

Mantini AR, Marzocchi MP, Smulevich G (1989) Raman excitation profiles and second derivative absorption spectra of B-carbonate. J Chem Phys 91:85–91

Markham JJ (1959) Interaction of normal modes with electron traps. Rev Mod Phys 31:956–989

Marquardt DW (1963) An algorithm for least-squares estimation of non linear parameters. J Soc Ind Appl Math 11:431–441

McMillin DR, Holwerda RA, Gray HB (1974a) Preparation and spectroscopic studies of Cobalt(II) derivatives of blue copper proteins. Proc Natl Acad Sci, USA 71:1339–1341

McMillin DR, Rosenberg RC, Gray HB (1974b) Preparation and spectroscopic studies of Cobalt(II) derivatives of blue copper proteins. Proc Natl Acad Sci, USA 71:4760–4762

Nestor L, Larrabee JA, Woolery G, Reinhammar B, Spiro TG (1984) Resonance raman spectra of blue copper proteins: assignments from normal mode calculations and copper-63/copper-65 and H_2O/D_2O shifts for Stellacyanin an Laccase. Biochemistry 23:1084–1093

Ruegg C, Lerch K (1981) Cobalt Tyrosinase: replacement of the binuclear copper of neurospora tyrosinase by cobalt. Biochemistry 20:1256–1262

Salvato B, Beltramini M (1990) Hemocyanins: molecular architecture, structure and reactivity of the binuclear copper active site. Life Chem Rep 8:1–47

Salvato B, Beltramini M, Piazzesi A, Alviggi M, Ricchelli F, Magliozzo RS, Peisach J (1986) Preparation, spectroscopic characterization and anion binding studies of a mononuclear Co(II) derivative of *Carcinus maenas* hemocyanin. Inorg Chim Acta 125:55–62

Salvato B, Beltramini M, Ricchelli F, Tallandini L (1989) Cobalt substitution studies on bovine erythrocyte superoxide dismutase: Evidence for a novel cobalt-superoxide dismutase derivative. Biochim Biophys Acta 998:14–20

Schomacker KT, Champion PM (1986) Investigations of spectral broadening mechanisms in biomolecules: Cytochrome-c. J Chem Phys 84:5314–5325

Solomon EI (1981) In: Spiro TG (ed) Copper proteins. John Wiley, New York

Solomon EI, Dooley DM, Wang RH, Gray HB, Cerdonio M, Mogno F, Romani GL (1975) Susceptibility studies of laccase and oxyhemocyanin using an ultrasensitive magnetometer. J Am Chem Soc 98:1029–1031

Solomon EI, Rawlings J, McMillin DR, Stephens PJ, Gray HB (1976) Infrared and visible circular dichroism and magnetic circular dichroism studies on cobalt(II)-substituted blue copper proteins. J Am Chem Soc 98:8046–8048

Solomon EI, Hare JW, Dooley DM, Dawson JH, Stephens PJ, Gray HB (1980) Spectroscopic studies of stellacyanin, plastocyanin and azurin. Electronic structure of the blue copper site. J Am Chem Soc 102:168–178

Solomon EI, Baldwin MJ, Lowery MD (1992) Electronic structures of active sites in copper proteins: contributions to reactivity. Chem Rev 92:521–542

Srajer V, Champion PM (1991) Investigations of optical line shapes and kinetic hole burning in myoglobin. Biochemistry 30:7390–7402

Srajer V, Schomacker KT, Champion PM (1986) Spectral broadening in biomolecules. Phys Rev Lett 52:1267–1270

Suzuki S, Hirose S, Savada S, Nakahara A (1985) Co(II)-substituted *Octopus vulgaris* Hemocyanin. Inorg Chim Acta 108:155–157

Thamann TJ, Loehr JS, Loehr TM (1977) Resonance raman study of oxyhemocyanin with unsymmetrically labeled oxygen. J Am Chem Soc 99:4187–4189

Volbeda A, Hol WGJ (1989) Crystal structure of hexameric haemocyanin from *Panurilus interruptus* refined at 3.2 Å resolution. J Mol Biol 209:249–279

Weakliem HA (1962) Optical spectra of Ni^{2+}, Co^{2+} and Cu^{2+} in tetrahedral sites in crystals. J Chem Phys 36:2117–2140

Woodruff WH, Norton KA, Swanson BI, Fry HA (1984) Temperature dependence of the resonance Raman spectra of plastocyanin and azurin between cryogenic and ambient conditions. Proc Natl Acad Sci, USA 81:1263–1267